

# Widely Separated Reduction Processes of abpy-Coupled Areneosmium(II) Reaction Centers (abpy = 2,2'-Azobispyridine): Stabilization of the Radical Intermediate and of the Os<sup>0</sup>Os<sup>II</sup> State

Frank Baumann and Wolfgang Kaim\*

Institut für Anorganische Chemie, Universität Stuttgart, Pfaffenwaldring 55,  
D-70550 Stuttgart, Germany

Gert Denninger and Hans-Jürgen Kümmerer

Physikalisches Institut, Universität Stuttgart, Pfaffenwaldring 57,  
D-70550 Stuttgart, Germany

Jan Fiedler

J. Heyrovský Institute of Physical Chemistry, Academy of Sciences of the Czech Republic,  
Dolejškova 3, CZ-18223 Prague, Czech Republic

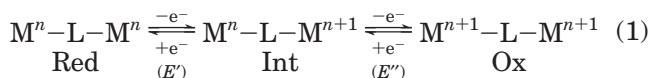
Received November 24, 2004

Electrochemical reactivity patterns have been established by cyclic voltammetry, EPR, and UV/vis spectroelectrochemistry for the transition [(C<sub>6</sub>Me<sub>6</sub>)ClOs]<sup>+</sup>/[(C<sub>6</sub>Me<sub>6</sub>)Os] in mono-nuclear and dinuclear complexes with the 2,2'-azobispyridine (abpy) and 2,2'-bipyrimidine (bpym) bridging ligands. The isolated electron reservoir intermediate {[(μ-abpy)[OsCl(C<sub>6</sub>Me<sub>6</sub>)<sub>2</sub>]<sup>+</sup>} could be analyzed by X band and W band EPR with regard to <sup>189</sup>Os hyperfine splitting and *g* anisotropy as an abpy anion radical species with significant contribution from the metal centers. The function of the π-conjugated acceptor ligand in mediating the interaction between two equivalent electron *and* atom transfer sites was analyzed through simulation of the cyclic voltammograms. In comparison with the system bridged by 2,2'-bipyrimidine, the dinuclear abpy complex displays a much stronger interaction between the two organometallic reaction centers, as illustrated by the 1.14 V vs 0.42 V splitting between the redox potentials separating the two chloride-dissociative processes, i.e., stabilizing the Os<sup>0</sup>Os<sup>II</sup> mixed-valent form [(Me<sub>6</sub>C<sub>6</sub>)Os(μ-abpy)OsCl(C<sub>6</sub>Me<sub>6</sub>)]<sup>+</sup>. This result parallels the observations made for (C<sub>5</sub>Me<sub>5</sub>)Rh- and (C<sub>5</sub>Me<sub>5</sub>)Ir-containing analogues and for the coupling of pure electron transfer centers through such bridging ligands.

## Introduction

The coupling of inorganic,<sup>1,2</sup> organometallic,<sup>3,4</sup> or main group element<sup>5,6</sup> electron transfer centers through π-conjugated molecular bridges has produced unusual molecular redox systems that have provided valuable insight into electron transfer reactivity. For instance, self-exchange can thus be approached as a structurally controlled degenerate *intramolecular* phenomenon in-

stead of as an intermolecular process.<sup>7</sup> As a side effect of such studies, new stable mixed-valent intermediates were obtained<sup>1–4,8</sup> that owe their existence to strong electronic communication between the electron transfer centers via mediating molecular bridges; degenerate half-wave potentials *E* for two such chemically identical centers may thus split into two different values *E'* and *E''*, the separation Δ*E* = *E'* – *E''* relating to the comproportionation constant *K<sub>c</sub>* (eq 1).<sup>2,8</sup>



$$\text{Comproportionation constant } K_c = \frac{[\text{Int}]^2}{[\text{Red}][\text{Ox}]} = 10^{\Delta E/59\text{mV}} \text{ (at 298 K)} \quad (2)$$

In an effort to extend this concept to *reaction centers* beyond mere electron transfer, i.e., to molecular frag-

(1) Prassides, K., Ed. *Mixed Valency Systems—Applications in Chemistry, Physics and Biology*; Kluwer Academic Publishers: Dordrecht, 1991.

(2) (a) Creutz, C. *Progr. Inorg. Chem.* **1983**, *30*, 1–73. (b) Richardson, D. E.; Taube, H. *Coord. Chem. Rev.* **1984**, *60*, 107–129. (c) Crutchley, R. J. *Adv. Inorg. Chem.* **1994**, *41*, 273–325. (d) Ward, M. D. *Chem. Soc. Rev.* **1995**, *34*, 121–134. (e) Demadis, K. D.; Hartshorn, C. M.; Meyer, T. J. *Chem. Rev.* **2001**, *101*, 2655–2685. (f) Glöckle, M.; Kaim, W.; Klein, A.; Roduner, E.; Hübner, G.; Zalis, S.; van Slageren, J.; Renz, F.; Gütllich, P. *Inorg. Chem.* **2001**, *40*, 2256–2262.

(3) Atwood, C. G.; Geiger, W. E.; Rheingold, A. L. *J. Am. Chem. Soc.* **1993**, *115*, 5310–5311.

(4) Bruns, W.; Kaim, W.; Waldhör, E.; Krejciik, M. *Inorg. Chem.* **1995**, *34*, 663–672.

(5) Fiedler, J.; Zalis, S.; Klein, A.; Hornung, F.; Kaim, W. *Inorg. Chem.* **1996**, *35*, 3039–3043.

(6) (a) Nelsen, S. F. *Chem. Eur. J.* **2000**, *6*, 581–588. (b) Lambert, C.; Nöll, G. *J. Am. Chem. Soc.* **1999**, *121*, 8434–8442.

(7) Taube, H. *Angew. Chem.* **1984**, *96*, 315–326; *Angew. Chem., Int. Ed. Engl.* **1984**, *23*, 329–388.

(8) Kaim, W.; Klein, A.; Glöckle, M. *Acc. Chem. Res.* **2000**, *33*, 755–763.

ments that undergo not only electron transfer processes (E) but electron transfer *and* chemical transformations, such as bond breaking, we have used organometallic reaction centers  $[(C_5Me_5)ClM]^+$ ,  $M = Rh$  or  $Ir$ , from hydride transfer catalysis,<sup>9</sup> which typically undergo a two-electron ECE reaction to  $[(C_5Me_5)M]$ , involving the reversible loss of chloride (C process).<sup>9,10</sup> As bridging ligands we used bis-chelating acceptor ligands such as 2,2'-bipyrimidine (bpym),<sup>11</sup> 3,6-bis(2-pyridyl)-1,2,4,5-tetrazine (bptz), and 2,5-bis(1-iminophenyl)pyrazine (bpi)<sup>12</sup> or 2,2'-azobipyridyl ligands.<sup>13</sup>



Related to  $[(C_5Me_5)ClM]^+$ ,  $M = Rh$  or  $Ir$ , are areneosmium cations  $[(C_6R_6)ClOs]^+$ , which have been studied with 2,2'-bipyridine (bpy) and bpym ligands.<sup>14,15</sup> For the latter, the dinuclear  $\{(\mu\text{-bpym})[OsCl(p\text{-Cym})]_2\}(PF_6)_2$ ,  $p\text{-Cym} = p\text{-cymene}$ , has been identified structurally in the *anti* (*trans*) configuration,<sup>15</sup> analysis of the cyclic voltammograms by simulation has also been performed, yielding a difference of 0.41 V between the two potentials related to the transformation  $[(\text{arene})ClOs]^+ \rightarrow [(\text{arene})Os]$ .<sup>15</sup> Considering the relatively poor interaction brought about by the bpym bridging ligand for electron transfer centers such as  $[(H_3N)_4Ru]^{2+/3+}$ ,<sup>16</sup>  $[(bpy)_2Ru]^{2+/3+}$ ,<sup>17</sup> or  $[(NC)_4Fe]^{-/2-}$ ,<sup>18</sup> we have now investigated the  $[(C_6Me_6)ClOs]^+ / [(C_6Me_6)Os]$  system in mononuclear and dinuclear complexes with bpym and the very strongly metal-metal coupling 2,2'-azobipyridine (abpy) ligand.<sup>13,19</sup>

Abpy can be conveniently synthesized by oxidative coupling of 2-aminopyridine and was early recognized to exhibit a strong interaction with low-valent metal centers such as iron(II) and to have a potential for several different coordination modes.<sup>19</sup> The structurally established alternatives include mono- and dinuclear coordination situations with the formation of five-membered chelate rings NNCNM. The ability of the abpy ligand to bridge two metal centers at a distance of about 5 Å, the small size of its  $\pi$  system, and the very low-lying  $\pi^*$  orbital make it a very special ligand,

suitable for studying metal-metal interaction across an unsaturated molecular bridge.<sup>19a</sup>

The compounds reported herein are mononuclear  $[(\text{abpy})OsCl(C_6Me_6)](PF_6)$  (**1**) and the dinuclear analogue that was initially isolated as one-electron-reduced (i.e., radical) species  $\{(\mu\text{-abpy})[OsCl(C_6Me_6)]_2\}(PF_6)$  (**2a**) but was then converted into  $\{(\mu\text{-abpy})[OsCl(C_6Me_6)]_2\}(PF_6)_2$  (**2b**). Cyclic voltammetric, UV-vis-spectroelectrochemical, and EPR characterization in the X and W band of the intermediates will be described, and the results obtained shall be compared to those of the bpym-bridged analogues **3**, **4**, and **4'**:<sup>15</sup>  $[(\text{abpy})OsCl(C_6Me_6)](PF_6)$  (**1**),  $\{(\mu\text{-abpy})[OsCl(C_6Me_6)]_2\}(PF_6)$  (**2a**),  $\{(\mu\text{-abpy})[OsCl(C_6Me_6)]_2\}(PF_6)_2$  (**2b**),  $[(\text{bpym})OsCl(C_6Me_6)](PF_6)$  (**3**),  $\{(\mu\text{-bpym})[OsCl(C_6Me_6)]_2\}(PF_6)_2$  (**4**),  $\{(\mu\text{-bpym})[OsCl(p\text{-Cym})]_2\}(PF_6)_2$  (**4'**).

## Experimental Section

**Instrumentation.** X band EPR spectra at about 9.5 GHz were recorded on a Bruker System ESP 300 equipped with a Bruker ER035M gaussmeter and a HP 5350B microwave counter. W band EPR spectra at about 94 GHz were obtained with a Bruker ELEX SYS E680 spectrometer. <sup>1</sup>H NMR spectra were taken on a Bruker AC 250 spectrometer. UV/vis absorption spectra were recorded on a Bruins Instruments Omega 10 spectrophotometer. Cyclic voltammetry was carried out at  $25 \pm 2$  °C under an atmosphere of dry argon in DMF/0.1 M Bu<sub>4</sub>NPF<sub>6</sub>, using a three-electrode configuration (glassy carbon working electrode, Pt counter electrode, Ag wire reference electrode) and a PAR 273 potentiostat and function generator. The ferrocene/ferrocenium couple served as internal reference. The program DigiSim 2.1<sup>20</sup> was used to reproduce cyclic voltammograms; cross reactions were not considered, and the diffusion coefficients were generally set to  $10^{-5}$  cm<sup>2</sup> s<sup>-1</sup> ( $\alpha = 0.5$ ). In situ radical generation for EPR spectroscopy was performed using a two-electrode cell,<sup>21a</sup> and an OTTL cell<sup>21b</sup> was used for UV/vis/NIR spectroelectrochemistry.

**$[(\text{abpy})OsCl(C_6Me_6)](PF_6)$  (**1**).** A 212 mg (0.25 mmol) amount of  $[(C_6Me_6)Cl_2Os]_2$ <sup>22</sup> was heated under reflux together with 110 mg (0.60 mmol) of abpy for 4 h in 75 mL of methanol. Filtration, reduction of the filtrate volume to 10 mL, addition of a concentrated solution of 387 mg (1.00 mmol) of Bu<sub>4</sub>NPF<sub>6</sub>, and finally cooling to 0 °C produced an orange-brown precipitate, which was washed with methanol and diethyl ether and dried under vacuum (202 mg, 56%). Anal. Calcd for C<sub>22</sub>H<sub>26</sub>ClF<sub>6</sub>N<sub>4</sub>OsP (717.7): C, 36.85; H, 3.65; N, 7.81. Found: C, 36.99; H, 3.58; N, 7.46. <sup>1</sup>H NMR (CD<sub>3</sub>NO<sub>2</sub>):  $\delta$  2.21 (s, 18H, C<sub>6</sub>Me<sub>6</sub>), 7.82 (ddd, 1H, H<sup>5</sup>), 7.79 (dt, 1H, H<sup>3</sup>), 8.05 (td, 1H, H<sup>5</sup>), 8.33 (td, 1H, H<sup>4</sup>), 8.35 (td, 1H, H<sup>4</sup>), 8.88 (ddd, 1H, H<sup>6</sup>), 8.94 (dt, 1H, H<sup>6</sup>), 8.95 (dt, 1H, H<sup>3</sup>) ppm. <sup>3</sup>J(H<sup>3</sup>H<sup>4</sup>) = 8.0 Hz, <sup>4</sup>J(H<sup>3</sup>H<sup>5</sup>) = 1.5 Hz, <sup>5</sup>J(H<sup>3</sup>H<sup>6</sup>) = 0.8 Hz, <sup>3</sup>J(H<sup>4</sup>H<sup>5</sup>) = 7.7 Hz, <sup>4</sup>J(H<sup>4</sup>H<sup>6</sup>) = 1.5 Hz, <sup>3</sup>J(H<sup>5</sup>H<sup>6</sup>) = 5.7 Hz, <sup>3</sup>J(H<sup>3</sup>H<sup>4</sup>) = 8.1 Hz, <sup>4</sup>J(H<sup>3</sup>H<sup>5</sup>) = 1.0 Hz, <sup>5</sup>J(H<sup>3</sup>H<sup>6</sup>) = 1.0 Hz, <sup>3</sup>J(H<sup>4</sup>H<sup>5</sup>) = 7.5 Hz, <sup>4</sup>J(H<sup>4</sup>H<sup>6</sup>) = 1.8 Hz, <sup>3</sup>J(H<sup>5</sup>H<sup>6</sup>) = 4.9 Hz.

**$\{(\mu\text{-abpy})[OsCl(C_6Me_6)]_2\}(PF_6)$  (**2a**).** A 212 mg (0.250 mmol) amount of  $[(C_6Me_6)Cl_2Os]_2$ <sup>22</sup> was heated under reflux together with 41 mg (0.225 mmol) of abpy for 12 h in 75 mL of methanol. Filtration, reduction of the filtrate volume to 10 mL, addition of a concentrated solution of 387 mg (1.00 mmol) of Bu<sub>4</sub>NPF<sub>6</sub>, and cooling to 0 °C produced a dark purple precipitate, which was washed with methanol and diethyl ether and

(9) Kölle, U.; Grätzel, M. *Angew. Chem.* **1987**, *99*, 572–574; *Angew. Chem., Int. Ed. Engl.* **1987**, *26*, 568–570.

(10) (a) Ladwig, M.; Kaim, W. *J. Organomet. Chem.* **1991**, *419*, 233–243. (b) Ladwig, M.; Kaim, W. *J. Organomet. Chem.* **1992**, *439*, 79–90.

(11) Kaim, W.; Reinhardt, R.; Greulich, S.; Sieger, M.; Klein, A.; Fiedler, J. *Collect. Czech. Chem. Commun.* **2001**, *66*, 291–306.

(12) Kaim, W.; Reinhardt, R.; Fiedler, J. *Angew. Chem.* **1997**, *109*, 2600–2602; *Angew. Chem., Int. Ed. Engl.* **1997**, *36*, 2493–2495.

(13) (a) Kaim, W.; Reinhardt, R.; Greulich, S.; Fiedler, J. *Organometallics* **2003**, *23*, 2240–2244. (b) Frantz, S.; Reinhardt, R.; Greulich, S.; Wanner, M.; Fiedler, J.; Duboc-Toia, C.; Kaim, W. *Dalton Trans.* **2003**, 3370–3375.

(14) Kaim, W.; Reinhardt, R.; Sieger, M. *Inorg. Chem.* **1994**, *33*, 4453–4459.

(15) Baumann, F.; Stange, A.; Kaim, W. *Inorg. Chem. Commun.* **1998**, *1*, 305–308.

(16) Baumann, F.; Kaim, W.; Garcia Posse, M.; Katz, N. E. *Inorg. Chem.* **1998**, *37*, 658–660.

(17) Ernst, S. D.; Kaim, W. *Inorg. Chem.* **1989**, *28*, 1520–1528.

(18) Glöckle, M.; Kaim, W.; Katz, N. E.; Garcia Posse, M.; Cutin, E.; Fiedler, J. *Inorg. Chem.* **1999**, *38*, 3270–3274.

(19) (a) Kaim, W. *Coord. Chem. Rev.* **2001**, *219–221*, 463–488. (b) Dogan, A.; Sarkar, B.; Klein, A.; Lissner, F.; Schleid, Th.; Fiedler, F.; Zalis, S.; Jain, V. K.; Kaim, W. *Inorg. Chem.* **2004**, *43*, 5973–5980.

(20) (a) *DigiSim 2.1*; Bioanalytical Systems: West Lafayette, IN. (b) Feldberg, S. W.; Goldstein, C. I.; Rudolph, M. *J. Electroanal. Chem.* **1996**, *413*, 25–36.

(21) (a) Kaim, W.; Ernst, S.; Kasack, V. *J. Am. Chem. Soc.* **1990**, *112*, 173–178. (b) Krejčík, M.; Danek, M.; Hartl, F. *J. Electroanal. Chem.* **1991**, *317*, 179–187.

(22) Kiel, W. A.; Ball, R. G.; Graham, W. A. G. *J. Organomet. Chem.* **1990**, *383*, 481–496.

dried under vacuum (173 mg, 73%). Anal. Calcd for  $C_{34}H_{44}Cl_2F_6N_4Os_2P$  (1105.0): C, 36.96; H, 4.01; N, 5.07. Found: C, 37.08; H, 4.02; N, 5.08.

$\{(\mu\text{-abpy})[\text{OsCl}(\text{C}_6\text{Me}_6)]_2\}(\text{PF}_6)_2$  (**2b**). A cooled solution of 20 mg (0.018 mmol) of **2a** in 10 mL of  $\text{CH}_3\text{CN}$  was treated with 10 mg (0.085 mmol) of solid  $\text{NOPF}_6$  for 1 h under a slight argon flow. After the color change from purple to green the solvent was removed, the residue redissolved in an ethanol/acetone (1:1) mixture, and a saturated solution of  $\text{Bu}_4\text{NPF}_6$  in ethanol added. The dark green precipitate was collected, washed with diethyl ether, and dried under vacuum (18 mg (80%). Anal. Calcd for  $C_{34}H_{44}Cl_2F_{12}N_4Os_2P_2$  (1249.9): C, 32.67; H, 3.55; N, 4.48. Found: C, 33.02; H, 3.67; N, 4.56.  $^1\text{H NMR}$  ( $\text{CD}_3\text{NO}_2$ ):  $\delta$  2.37 (s, 18H,  $\text{C}_6\text{Me}_6$ ), 8.13 (ddd, 1H,  $\text{H}^{5,5}$ ), 8.43 (td, 1H,  $\text{H}^{4,4}$ ), 8.74 (d, 1H,  $\text{H}^{3,3}$ ), 9.01 (d, 1H,  $\text{H}^{6,6}$ ) ppm.  $^3J(\text{H}^3\text{H}^4) = 8.5$  Hz,  $^4J(\text{H}^3\text{H}^5) = 7.4$  Hz,  $^3J(\text{H}^4\text{H}^5) = 7.5$  Hz,  $^4J(\text{H}^4\text{H}^6) = 1.4$  Hz,  $^3J(\text{H}^5\text{H}^6) = 5.6$  Hz.

$[(\text{bpym})\text{Os}(\text{C}_6\text{Me}_6)](\text{PF}_6)$  (**3**). A procedure similar to that for the synthesis of **1** yielded 243 mg (70%). Anal. Calcd for  $C_{20}H_{24}ClF_6N_4OsP$  (691.1): C, 34.76; H, 3.50; N, 8.11. Found C, 34.58; H, 3.36; N, 8.09.  $^1\text{H NMR}$  ( $\text{CD}_3\text{NO}_2$ ):  $\delta$  2.31 (s, 18H,  $\text{C}_6\text{Me}_6$ ), 8.01 (dd, 2H,  $\text{H}^{5,5}$ ), 9.20 (dd, 2H,  $\text{H}^{4,4}$ ), 9.25 (dd, 2H,  $\text{H}^{6,6}$ ) ppm.  $^3J(\text{H}^4\text{H}^5) = 4.8$  Hz,  $^3J(\text{H}^5\text{H}^6) = 5.9$  Hz,  $^4J(\text{H}^4\text{H}^6) = 2.0$  Hz.

$\{(\mu\text{-bpym})[\text{OsCl}(\text{C}_6\text{Me}_6)]_2\}(\text{PF}_6)_2$  (**4**). A procedure similar to that for the synthesis of **2a** yielded 257 mg (84%). Anal. Calcd for  $C_{32}H_{42}Cl_2F_{12}N_4Os_2P_2$  (1224.0): C, 31.40; H, 3.46; N, 4.58. Found: C, 31.38; H, 3.46; N, 4.54.  $^1\text{H NMR}$  ( $\text{CD}_3\text{NO}_2$ ):  $\delta$  2.34 and 2.39 (s, 36H,  $\text{C}_6\text{Me}_6$ ), 8.30 and 8.28 (t, 2H,  $\text{H}^{5,5}$ ), 9.32 and 9.29 (d, 4H,  $\text{H}^{4,4,6,6}$ ) ppm (mixture of *syn* and *anti* isomers in a 2:1 ratio).  $^3J(\text{H}^4\text{H}^5) = 5.8$  Hz.

## Results and Discussion

**Synthesis and Configuration.** The compounds  $[(\text{abpy})\text{OsCl}(\text{C}_6\text{Me}_6)](\text{PF}_6)$  (**1**) and  $\{(\mu\text{-abpy})[\text{OsCl}(\text{C}_6\text{Me}_6)]_2\}(\text{PF}_6)_2$  (**2a**) were obtained as air-stable species by reaction of the abpy ligand with  $[(\text{C}_6\text{Me}_6)\text{Cl}_2\text{Os}]_2$  in methanol. The rather positive reduction potential of the dinuclear system (cf. below) caused the initial formation<sup>23</sup> of the paramagnetic one-electron-reduced species **2a**, from which the diamagnetic  $\{(\mu\text{-abpy})[\text{OsCl}(\text{C}_6\text{Me}_6)]_2\}(\text{PF}_6)_2$  (**2b**) could be obtained by oxidation with  $\text{NOPF}_6$ .

As outlined previously,<sup>11,13,15</sup> dinuclear systems such as **2** or **4** can exist as diastereoisomers with the two chloride ligands in either *syn* or *anti* (*cis* or *trans*) positions relative to the plane of the bridging ligand. For  $\{(\mu\text{-bpym})[\text{OsCl}(p\text{-Cym})]_2\}(\text{PF}_6)_2$  (**4'**) an *anti* position was established crystallographically,<sup>15</sup> and compound **4** was isolated as a 2:1 mixture of isomers. In contrast, the complex dication of **2b** exists in only one configuration according to the  $^1\text{H NMR}$  spectrum; by analogy and considering the typically smaller metal–metal distances  $d < 5.1$  Å in abpy-bridged dimers<sup>24</sup> relative to bpym-bridged dinuclear species (cf.  $d_{\text{Os-Os}} = 5.674(1)$  Å in **4'**)<sup>15</sup> we assume this to be the *anti* (*trans*) isomer. That *anti* isomer of **2** would be the *meso* form, as the metals in **1** and **2** are centers of chirality; the strongly electron-accepting azo nitrogen atoms of abpy are electronically quite different from the more basic but less  $\pi$ -acidic pyridyl nitrogen atoms.<sup>19</sup>

(23) The oxidized component of that reaction, presumably a high-valent osmium species, has not been isolated. Cf. e.g.: Sixt, T.; Kaim, W.; Preetz, W. *Z. Naturforsch.* **2000**, *55b*, 235. Alternatively, the solvent can act as a reducing component.

(24) Hartmann, H.; Scheiring, T.; Fiedler, J.; Kaim, W. *J. Organomet. Chem.* **2000**, *604*, 267–272.

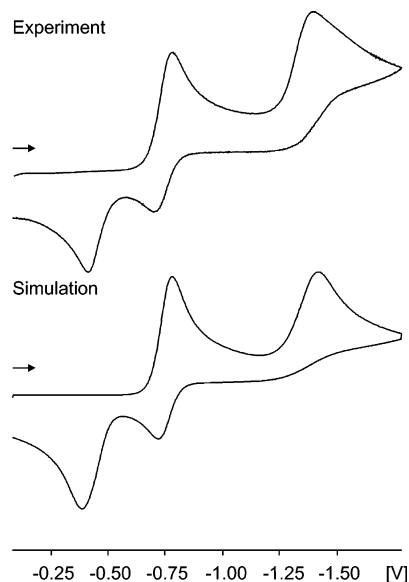


**Figure 1.** Cyclic voltammogram of  $[(\text{C}_6\text{Me}_6)\text{OsCl}(\text{abpy})](\text{PF}_6)$  (**1**) in 0.1 M  $\text{Bu}_4\text{NPF}_6/\text{DMF}$  at 250 mV/s scan rate (top) and simulation with the data from Table 1 (bottom).

**Reduction of the Mononuclear Complex 1.** The prototypical mononuclear complex ions  $[(\text{bpy})\text{OsCl}(\text{C}_6\text{Me}_6)]^+$  and  $[(\text{bpym})\text{OsCl}(\text{C}_6\text{Me}_6)]^+$  exhibit a two-electron reduction behavior with concomitant loss of chloride,<sup>14,15</sup> similarly to the related complex ions  $[(\alpha\text{-diimine})\text{MCl}(\text{C}_5\text{Me}_5)]^+$ ,  $\text{M} = \text{Rh}$  or  $\text{Ir}$ .<sup>9,10</sup> These processes were attributed to metal-based electron uptake in an ECE or EEC mechanism (E: one-electron transfer at the electrode; C: chemical step, here: chloride dissociation).<sup>10,14,15</sup> Although apparently irreversible in cyclic voltammetry, these two-electron processes are chemically reversible; that is, reoxidation at positive potential leads back to the original species. A detailed study of the 3d transition metal analogue  $[(\text{bpy})(\text{C}_5\text{Me}_5)\text{ClCo}]^+$  has shown that the two-electron reaction is split into a chloride-dissociative first one-electron reduction to yield  $[(\text{bpy})(\text{C}_5\text{Me}_5)\text{Co}^{\text{II}}]^+$  and a subsequent reversible one-electron process.<sup>25</sup>

In contrast to  $[(\text{bpym})\text{OsCl}(\text{C}_6\text{Me}_6)](\text{PF}_6)$  (**3**) or  $[(\text{bpym})\text{OsCl}(p\text{-Cym})](\text{PF}_6)$ ,<sup>15</sup> the mononuclear **1** with the much stronger  $\pi$ -acceptor ligand abpy is reduced via *two consecutive one-electron steps*. Analysis of the cyclic voltammogram (Figure 1) shows the first step to be electrochemically reversible with only slow loss of chloride, whereas the second step is strongly dissociative with respect to the  $\text{Cl}^-$  ligand. EPR results (cf. below) confirm that the first electron occupies a largely abpy ligand-centered MO, which explains the difference between the bpy/cobalt (rapid  $\text{Cl}^-$  dissociation)<sup>25</sup> and abpy/osmium systems (slow  $\text{Cl}^-$  dissociation). In the latter case, the charge is stored in the acceptor ligand, which renders this form a (chemically inactive) electron reservoir intermediate (electron accumulation effect).<sup>26</sup> Only after addition of the *second* electron does rapid chloride dissociation occur; that is, both electrons then combine to create a formal osmium(0) species  $[(\text{abpy})-$

(25) Kaim, W.; Reinhardt, R.; Waldhör, E.; Fiedler, J. *J. Organomet. Chem.* **1996**, *524*, 195–202.

(26) Kaim, W. In *New Trends in Molecular Electrochemistry*; Pombeiro, A. J. L., Ed.; Fontis Media: Lausanne, 2004; pp 127–151.

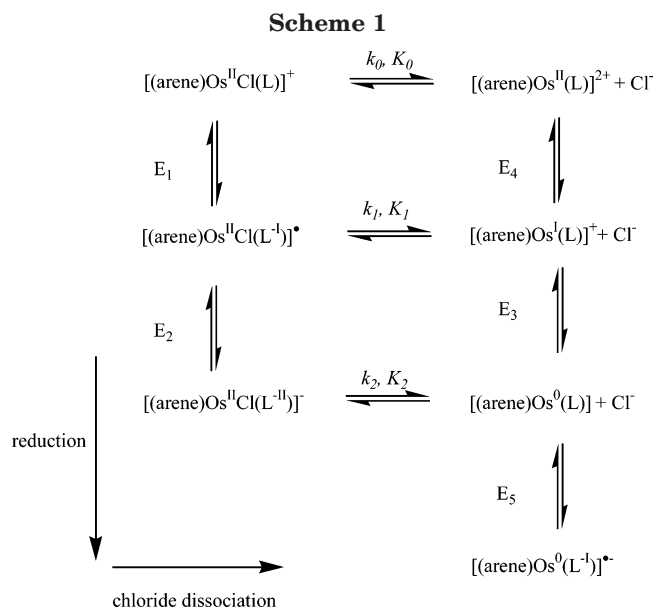


**Table 1. Half-Wave Potentials  $E_i^a$ , Rate Constants  $k_j^b$ , and Equilibrium Constants  $K_j^c$  for the Reduction of the Complexes  $[(C_6Me_6)OsCl(L)](PF_6)^{d,e}$**

i	1	2	3	4	5 <sup>f</sup>
$E_i$	-0.74 (-1.36)	-1.31 (-1.67)	-0.46 (-1.01)	-0.40 (-1.01)	-2.66 (-2.56)
j	0	1	2		
$k_j$	$g$ ( $g$ )		$0.10 \pm 0.02$ ( $2.0 \pm 0.2$ )	$>1000^h$ ( $>1000^h$ )	
$K_j$	$1 \times 10^{-12i}$ ( $2 \times 10^{-6j}$ )		$0.1 \pm 0.05$ ( $0.5 \pm 0.1$ )	$6 \times 10^{6i}$ ( $4 \times 10^{12j}$ )	

<sup>a</sup> In V vs ferrocenium/ferrocene. <sup>b</sup> In  $s^{-1}$ . <sup>c</sup> In mol/L. <sup>d</sup> Heterogeneous electron transfer rates set at  $1 \text{ cm}^2 \text{ s}^{-1}$ , except for step 2 ( $k_{si} = 0.001$  for L = abpy and 0.008 for L = bpym). <sup>e</sup> From simulation of the cyclic voltammograms obtained at 250 mV/s (L = abpy) or 1 V/s (L = bpym) in 0.1 M  $Bu_4NPF_6/DMF$  (Scheme 1). Values for L = abpy, values for L = bpym in parentheses. <sup>f</sup> Determined directly. <sup>g</sup> Set at  $0.1 \text{ s}^{-1}$ . <sup>h</sup> From fast scan measurements. <sup>i</sup> Dependent variable (thermodynamically superfluous reaction<sup>20</sup>).

$Os(C_6Me_6)$ . While the actual electron distribution<sup>27</sup> may not correspond to that simplistic oxidation state formulation due to strong  $\pi$ -back-donation from  $Os^0$  to the excellent  $\pi$  acceptor abpy even in the ground state, the lowered coordination number of the metal is in agreement with significant electron acquisition by the transition metal.

For a more quantitative assessment, the cyclic voltammograms of **1** and **3** have been simulated (Figure 1, Scheme 1, Table 1). This approach<sup>26</sup> revealed a labilization of the chloride even after the first electron uptake with a quite pronounced effect for the bpym analogue **3** with its more negative potentials (Table 1). In contrast, the value of  $k_1 = 0.1 \text{ s}^{-1}$  leaves sufficient time for characterization of the chloride-containing intermediate  $[(abpy)OsCl(C_6Me_6)]^*$ , the stability of which is further enhanced by addition of excess chloride.

EPR spectroscopy of in situ generated  $[(abpy)OsCl(C_6Me_6)]^*$  confirms the notion of a predominantly abpy ligand-centered first reduction of **1**. At room tempera-

ture in DMF/0.1 M  $Bu_4NCl$  there is an unresolved broad line ( $\Delta H = 2.7 \text{ mT}$ ) at  $g_{iso} = 1.9713$  for the neutral complex, which splits into two  $g$  components of an axial system in the glassy frozen state (Table 2). The notable deviation from  $g(\text{electron}) = 2.0023$  or  $g(\text{abpy}^{\bullet-}) = 2.0044$  can be attributed to the large spin-orbit coupling contribution from divalent osmium ( $\xi \approx 2500 \text{ cm}^{-1}$ ).<sup>28,29a</sup> The deviation to lower  $g$  values signifies the presence of low-lying unoccupied orbitals close to the singly occupied MO (SOMO),<sup>30</sup> possibly the low-lying metal  $d$  orbital involved in reductive chloride labilization. The related complex  $[(abpy)IrCl(C_5Me_5)]^*$  exhibits slightly higher  $g_{iso}$  and  $\Delta g = g_1 - g_3$  values (Table 2).<sup>13</sup>

UV/vis spectroelectrochemistry using an optically transparent thin-layer electrolytic (OTTLE) cell<sup>20</sup> was again used to characterize **1** and its one- and two-electron reduction products (Scheme 1). The persistence of the chloride-containing one-electron-reduced form  $[(abpy)OsCl(C_6Me_6)]^*$  was ensured by using 0.1 M  $Bu_4NCl/DMF$  as electrolyte. The spectrum of unreduced **1** (Figure 2, Table 3) shows singlet and less intense long-wavelength triplet ligand-to-metal charge transfer (LMCT) transitions involving the 5d element with its high spin-orbit coupling constant. DFT calculations on the  $[(bpy)IrCl(C_5H_5)]^+$  model system have confirmed this assignment.<sup>27</sup> Comparison between complex ions  $[(\alpha\text{-diimine})MCl(C_5Me_5)]^+$  (M = Rh or Ir) has shown the significance of the 5d configuration in allowing term-forbidden transitions such as singlet-triplet by virtue of the mixing through spin-orbit coupling.<sup>13,14</sup>

One-electron reduction to  $[(abpy)OsCl(C_6Me_6)]^*$  results in some intensity loss of the CT bands, while the SOMO-involving bands of the abpy radical anion<sup>20,31</sup> ligand become observable (Table 3). The following EC reduction to an "osmium(0)" species  $[(abpy)Os(C_6Me_6)]$  causes the CT bands to disappear and produces the expected<sup>14,15</sup>  $d(Os^0) \rightarrow \pi^*$  "MLCT" band in the visible region (Figure 2, Table 3). The latter probably involves highly mixed  $d_{xz}$  and  $\pi^*(\text{abpy})$  orbitals, as was similarly postulated for the analogous  $[(bpy)Os(C_6Me_6)]^{14}$  and as was confirmed by DFT calculation for the related  $[(bpy)Ir(C_5H_5)]$ .<sup>27</sup>

**Reduction of the Dinuclear Complex 2b.** The dinuclear system **2** exhibits a first reversible one-electron reduction (E) from **2b** to **2a**, followed by a chloride dissociative EC process to yield the "two-electron mixed-valent species"  $[(C_6Me_6)ClOs(\mu\text{-abpy})Os(C_6Me_6)]^+$ . In that respect, it is similar to **1** except for the much less negative potentials and the higher stability of the primarily reduced "electron-reservoir" intermediate **2a**.<sup>26</sup> This intermediate is capable of storing the first added electron without causing appreciable chloride dissociation (see  $k_j$  values, Table 4); only after accumulation of *two* electrons is there a rapid chemical reaction. The cyclic voltammogram for **2b** is shown together with the simulation in Figure 3; the

(28) Weil, J. A.; Bolton, J. R.; Wertz, J. E. *Electron Paramagnetic Resonance*; Wiley: New York, 1994.

(29) (a) Kober, E. M.; Meyer, T. J. *Inorg. Chem.* **1984**, *23*, 3877–3886. (b) Pramanik, K.; Shivakumar, M.; Ghosh, P.; Chakravorty, A. *Inorg. Chem.* **2000**, *39*, 195–199.

(30) Kaim, W. *Coord. Chem. Rev.* **1987**, *76*, 187–235.

(31) Krejci, M.; Zalis, S.; Klima, J.; Sykora, D.; Matheis, W.; Klein, A.; Kaim, W. *Inorg. Chem.* **1993**, *32*, 3362–3368.

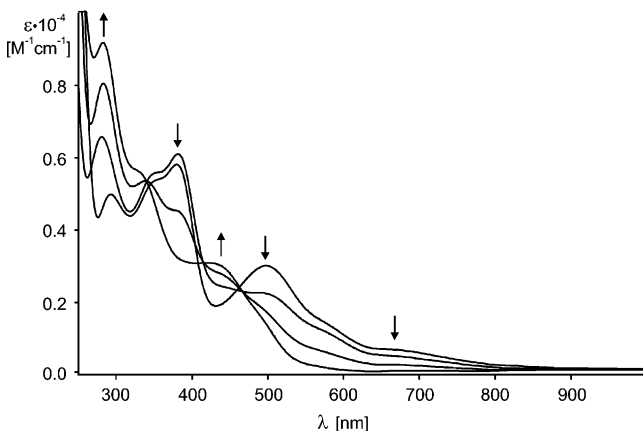
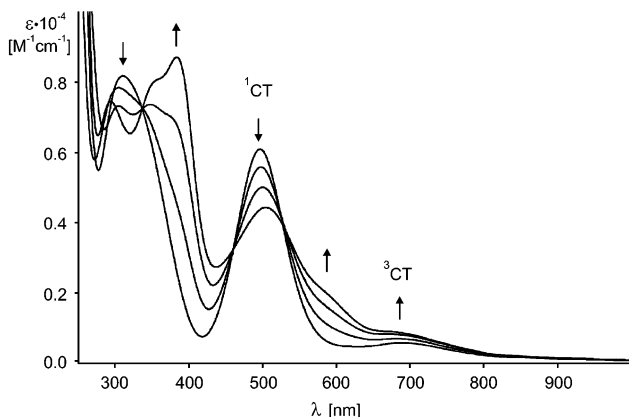
(27) Zalis, S.; Sieger, M.; Greulich, S.; Stoll, H.; Kaim, W. *Inorg. Chem.* **2003**, *42*, 5185–5191.

**Table 2. ESR Data of Mononuclear Radical Complexes**

complex	$g_{iso}^a$	$g_1^b$	$g_2^b$	$g_3^b$	$g_1 - g_3$	solvent	ref
$[(C_6Me_6)OsCl(abpy)]^{\bullet}$	1.9713	1.9893	1.9893	1.9643	0.025	DMF	this work
$[(C_5Me_5)IrCl(abpy)]^{\bullet}$	1.983	1.995	1.995	1.966	0.029	CH <sub>3</sub> CN	13a
$[(C_5Me_5)RhCl(abpy)]^{\bullet}$	1.998	1.998	1.998	1.998	<0.01	CH <sub>3</sub> CN	13a

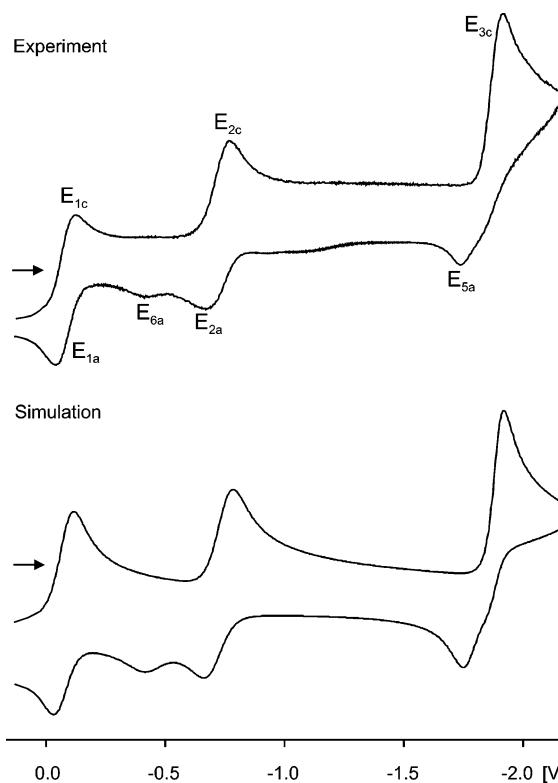
<sup>a</sup> At 298 K. <sup>b</sup> At 110 K.**Table 3. UV/Vis/NIR Data for  $[(C_6Me_6)OsCl(abpy)]^+$  and Reduction Products<sup>a</sup>**

complex	$\lambda_{max}$ [nm] ( $\epsilon \times 10^{-3}$ [M <sup>-1</sup> cm <sup>-1</sup> ])	assignment
$[(C_6Me_6)OsCl(abpy)]^+$	311 (8.1)	$\pi-\pi^*$
	496 (6.0)	<sup>1</sup> LLCT/MLCT
	690 (0.6)	<sup>3</sup> LLCT/MLCT
$[(C_6Me_6)OsCl(abpy)]^{\bullet}$	297 (7.2)	IL
	352sh	
	395 (8.6)	IL ( $\pi_7-\pi_8^*$ )
	505 (4.4)	<sup>1</sup> LLCT/MLCT
	581sh	IL ( $\pi_8^*-\pi_9^*$ )
$[(C_6Me_6)Os(abpy)]$	679 (0.9)	<sup>3</sup> LLCT/MLCT
	291 (11.0)	IL
	332sh	IL
	437 (8.6)	MLCT II
	492sh (1.8)	MLCT I

<sup>a</sup> From spectroelectrochemistry in DMF/0.1 M Bu<sub>4</sub>NPF<sub>6</sub>.**Figure 2.** Spectroelectrochemical response on reduction of  $[(C_6Me_6)OsCl(abpy)]^+$  to  $[(C_6Me_6)OsCl(abpy)]^{\bullet}$  (top) and further to  $[(C_6Me_6)Os(abpy)]$  (bottom) in 0.1 M Bu<sub>4</sub>NCl/DMF.

data according to the extended "ladder" Scheme 2<sup>32</sup> are summarized in Table 4.

The second metal reduction, on the other hand, proceeds in the rapid, dissociative two-electron fashion,

(32) Glöckle, M.; Fiedler, J.; Kaim, W. *Z. Anorg. Allg. Chem.* **2001**, *627*, 1441–1453.**Figure 3.** Cyclic voltammogram of  $\{(\mu\text{-abpy})[(C_6Me_6)\text{OsCl}]_2\}(\text{PF}_6)_2$  (**2b**) in 0.1 M Bu<sub>4</sub>NPF<sub>6</sub>/DMF at 100 mV/s scan rate (top) and simulation with the data from Table 4 (bottom).

as familiar from the simple mononuclear species such as **3**.<sup>14</sup> No osmium(I)-containing mixed-valent intermediate has been observed by EPR or absorption spectroscopy in contrast to ruthenium(I) in the related  $\{(\mu\text{-abpy})[(\text{arene})\text{Ru}]_2\}^+$ ,<sup>36</sup> the reason probably being a more pronounced reluctance to adopt the 5d<sup>7</sup> (Os<sup>I</sup>) configuration instead of 4d<sup>7</sup> (Ru<sup>I</sup>). This process leading to neutral  $(\mu\text{-abpy})[\text{Os}(C_6Me_6)]_2$  occurs at a rather negative potential, causing an effective splitting of  $E_2 - E_3 = -0.73 \text{ V} - (-1.87 \text{ V}) = 1.14 \text{ V}$  between the first and the second *chemical* (EC) step at the chosen scan rate of 100 mV/s. This splitting is thus much larger than the 0.42 V measured for the analogous bpym-bridged system **4** (Table 4) or for **4'**.<sup>15</sup> As shown previously,<sup>14</sup> the change from *p*-cymene to hexamethylbenzene arene ligands results in a slight cathodic shift of potentials. The

(33) Glöckle, M.; Kaim, W.; Katz, N. E.; Garcia Posse, M.; Cutin, E.; Fiedler, J. *Inorg. Chem.* **1999**, *38*, 3270–3274.(34) (a) Frantz, S.; Hartmann, H.; Doslik, N.; Wanner, M.; Kaim, W.; Kümmerer, H.-J.; Denninger, G.; Barra, A.-L.; Duboc-Toia, C.; Fiedler, J.; Ciofini, I.; Urban, C.; Kaupp, M. *J. Am. Chem. Soc.* **2002**, *124*, 10563–10571. (b) Kaim, W.; Kohlmann, S.; Jordanov, J.; Fenske, D. *Z. Anorg. Allg. Chem.* **1991**, *598/599*, 217–234. (c) Kaim, W.; Kohlmann, S. *Inorg. Chem.* **1987**, *26*, 68–77. (d) Kaim, W.; Kohlmann, S. *Inorg. Chem.* **1986**, *25*, 3442–3448.(35) Barra, A.-L.; Brunel, L.-C.; Baumann, F.; Schwach, M.; Moscherosch, M.; Kaim, W. *J. Chem. Soc., Dalton Trans.* **1999**, 3855–3857.(36) Sarkar, B.; Kaim, W.; Fiedler, J.; Duboc, C. *J. Am. Chem. Soc.* **2004**, *126*, 14707–14708.

## Scheme 2

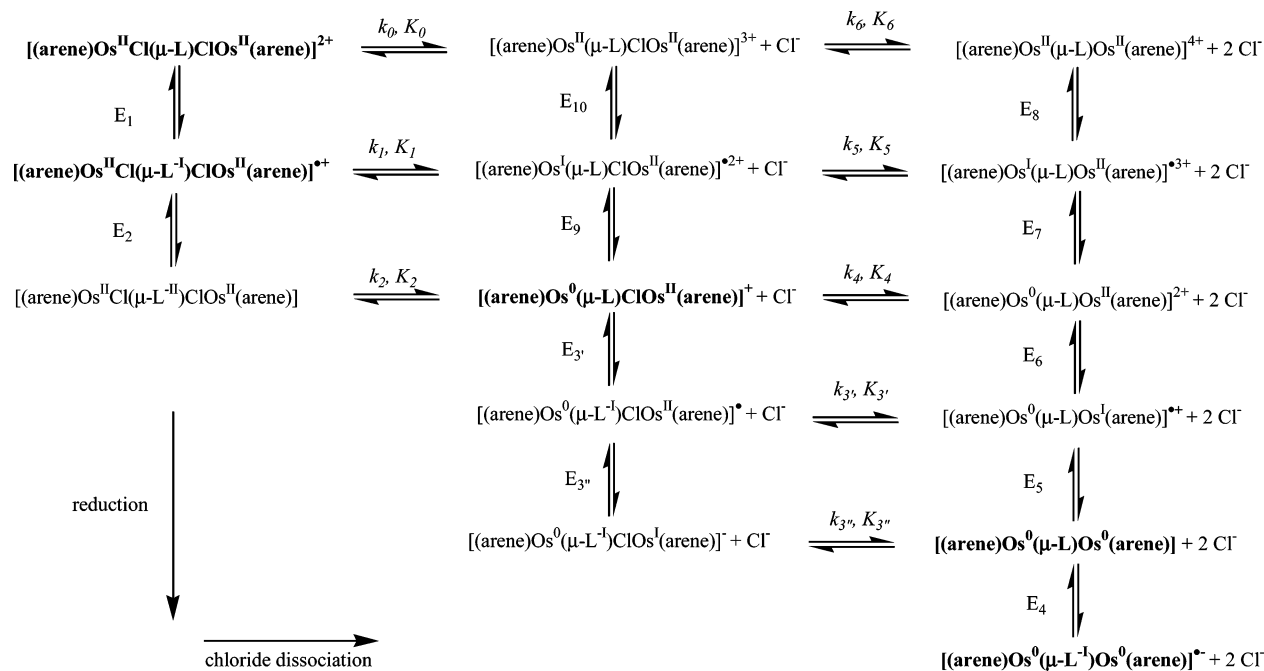


**Table 4. Half-Wave Potentials  $E_i$ ,<sup>a</sup> Rate Constants  $k_j$ ,<sup>b</sup> and Equilibrium Constants  $K_j$ <sup>c</sup> for the Reduction of Complexes  $\{(\mu\text{-L})[(\text{C}_6\text{Me}_6)\text{OsCl}]_2\}(\text{PF}_6)_2$ <sup>d,e</sup>**

i	1	2	3'	3''	4 <sup>f</sup>
$E_i$ [V]	-0.07 (-0.76)	-0.73 (-1.38)	-1.87 (-1.80)	-1.90 (-1.80)	-2.75 (-2.80)
i	5	6	7	8	9
$E_i$ [V]	-1.77 (-1.41)	-0.52 (-0.73)	<sup>g</sup> (-0.71)	<sup>g</sup> (-0.69)	-0.31 (-0.53)
j	0	1	2	3'	3''
$k_j$	<i>h</i> ( <i>h</i> )	<i>h</i> ( <i>h</i> )	$5 \pm 1$ ( $> 10^3$ )	<i>h</i> ( <i>h</i> )	$12 \pm 3$ $8 \pm 2$
$K_j$	$10^{-7i}$ ( $10^{-19j}$ )	$10^{-5i}$ ( $10^{-12j}$ )	$1 \pm 0.2$ ( $> 10^2$ )	$10^{-1i}$ ( $10^{-2}$ )	$> 100$ ( $200 \pm 50$ )

<sup>a</sup> In V vs ferrocenium/ferrocene. <sup>b</sup> In  $\text{s}^{-1}$ . <sup>c</sup> In mol/L. <sup>d</sup> Heterogeneous electron transfer rates set at  $1 \text{ cm}^2 \text{ s}^{-1}$ . <sup>e</sup> From simulation of the cyclic voltammograms obtained at 250 mV/s (L = abpy) or 100 mV/s (L = bpy) in 0.1 M  $\text{Bu}_4\text{NPF}_6/\text{DMF}$  (Scheme 2). Values for L = abpy, values for L = bpy in parentheses. <sup>f</sup> Determined directly. <sup>g</sup> Not observed. <sup>h</sup> Set at  $0.1 \text{ s}^{-1}$ . <sup>i</sup> Dependent variable (thermodynamically superfluous reaction<sup>20</sup>).

**Table 5. Reduction Potentials<sup>a</sup> for the Reduction of 2,2'-Bipyridine and 2,2'-Azobispyridine and of Some of Their Metal Complexes (L)(ML'<sub>n</sub>)<sub>k</sub>**

ML' <sub>n</sub>	L = bpy, $k = 1$	L = abpy, $k = 2$
$\text{Re}(\text{CO})_3\text{Cl}$	-1.70 (DMF)	+0.01 (DCE)
$[\text{Cu}(\text{PPh}_3)_2]^+$	-1.86 (DMF)	-0.28 ( $\text{CH}_2\text{Cl}_2$ )
$\text{Mo}(\text{CO})_4$	-1.86 (DMF)	-0.42 (DMF)
—	-2.55 (DMF) <sup>19a</sup>	-1.37 (DMF) <sup>19a</sup>
$\text{Rh}(\text{C}_5\text{Me}_5)$	-2.61 ( $\text{CH}_3\text{CN}$ ) <sup>14</sup>	-2.34 <sup>b</sup> ( $\text{CH}_3\text{CN}$ ) <sup>13</sup>
$\text{Ir}(\text{C}_5\text{Me}_5)$	-2.82 ( $\text{CH}_3\text{CN}$ ) <sup>14</sup>	-2.49 <sup>b</sup> ( $\text{CH}_3\text{CN}$ ) <sup>13</sup>
$\text{Os}(\text{C}_6\text{Me}_6)$	-3.00 <sup>b</sup> ( $\text{CH}_3\text{CN}$ ) <sup>14</sup>	-2.75 <sup>b</sup> (DMF)

<sup>a</sup> Potentials in V vs ferrocenium/ferrocene. <sup>b</sup> Cathodic peak potentials from cyclic voltammetry at 100 mV/s.

separation of 1.14 V is also larger than that observed for abpy-bridged dinuclear species involving the related  $(\text{C}_5\text{Me}_5)\text{ClRh}^+$  (0.75 V) or  $(\text{C}_5\text{Me}_5)\text{ClIr}^+$  (1.02 V) cations.<sup>13b</sup> Both the presumably somewhat closer metal–metal distance and the more efficient metal–metal interaction

mediation by abpy versus bpy can be considered responsible for the bridge effect; in agreement with previous arguments we assume that the latter is more important.<sup>32</sup> The special mediating capability of abpy as demonstrated also in mixed-valence chemistry<sup>19a,33</sup> is attributable to the low-lying  $\pi^*$  MO ( $b_g$ ), which has about 80% contribution from the nitrogen atoms interfacing with the metal centers in dinuclear compounds.<sup>19a</sup>

A further reversible one-electron reduction step was observed at a very negative potential of -2.75 V to yield the anionic  $\{(\mu\text{-abpy})[\text{Os}(\text{C}_6\text{Me}_6)]_2\}^-$  (Table 4). Characteristically, this potential is much more negative than that of free abpy at -1.37 V vs  $\text{Fc}^{+/0}$ ,<sup>19a</sup> confirming the substantial metal-to-ligand electron transfer in the ground state of neutral  $(\mu\text{-abpy})[\text{Os}(\text{C}_6\text{Me}_6)]_2$ . In fact, this potential is more negative even than the values determined for the related systems  $\{(\mu\text{-abpy})\text{-}[\text{M}(\text{C}_5\text{Me}_5)]_2\}^{0/-}$ ,<sup>13</sup> not to mention the abpy-bridged dinuclear complexes of rhenium(I), copper(I), or molybdenum(0).<sup>34</sup> Table 5 illustrates for both mononuclear bpy and dinuclear abpy complexes that hexamethylbenzeneosmium(0) is the strongest  $\pi$  donor fragment within the whole series.

The other parameters from Table 4 illustrate the expected dependence of rate and equilibrium constants for chloride dissociation on the oxidation states as well

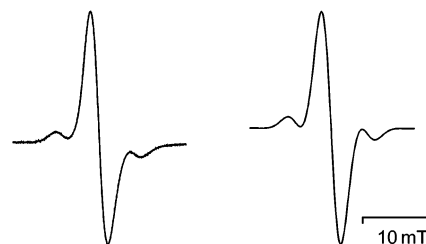


**Figure 4.** X band EPR spectrum of  $\{(\mu\text{-abpy})[(\text{C}_6\text{Me}_6)\text{-OsCl}]_2\}(\text{PF}_6)_2$  (**2a**) in 0.1 M  $\text{Bu}_4\text{NPF}_6/\text{DMF}$  at 298 K (left) and simulation with  $a(^{189}\text{Os}) = 3.5 \text{ mT}$  (line width 2.8 mT, right).

**Table 6.** EPR Data of Dinuclear Complexes of *abpy*<sup>−</sup>

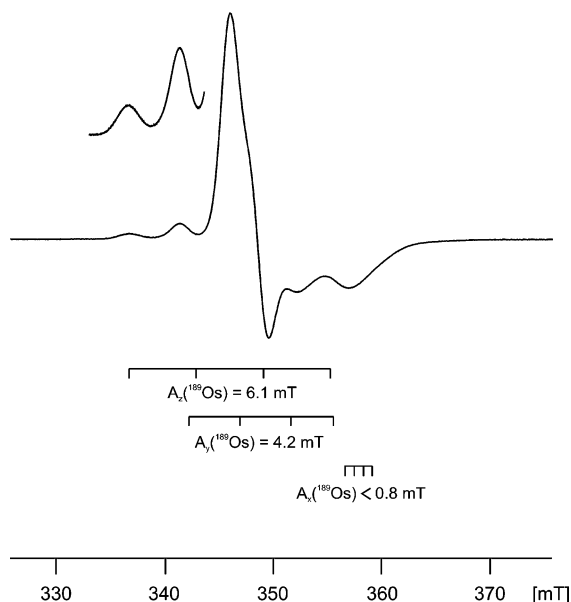
complex (L = <i>abpy</i> )	$g_{iso}^a$	$g_1^b$	$g_2^b$	$g_3^b$	$g_1 - g_3$	solvent	ref
{( $\mu$ -L)[(C <sub>6</sub> Me <sub>6</sub> )OsCl] <sub>2</sub> } <sup>•+</sup>	1.9515 <sup>c</sup>	1.9782 <sup>d</sup>	1.9631 <sup>e</sup>	1.9155	0.063	DMF	this work
{( $\mu$ -L)[(C <sub>5</sub> Me <sub>5</sub> )RhCl] <sub>2</sub> } <sup>•+</sup>	1.993	1.996	1.993	1.990	0.006	CH <sub>3</sub> CN <sup>h</sup>	13b
{( $\mu$ -L)[(C <sub>5</sub> Me <sub>5</sub> )IrCl] <sub>2</sub> } <sup>•+</sup>	1.968	1.979	1.971	1.954	0.025	CH <sub>3</sub> CN <sup>h</sup>	13b
{( $\mu$ -L)[Ru(Cym) <sub>2</sub> ] <sub>2</sub> } <sup>•+</sup>	1.989	1.9990	1.9886	1.9780	0.021	CH <sub>3</sub> CN <sup>h</sup>	36
{( $\mu$ -L)[W(CO) <sub>4</sub> ] <sub>2</sub> } <sup>•−</sup>	2.0089 <sup>f</sup>	<i>g</i>	<i>g</i>	<i>g</i>	<i>g</i>	THF	34d
{( $\mu$ -L)[Re(CO) <sub>3</sub> Cl] <sub>2</sub> } <sup>•−</sup>	2.0039	2.023	2.007	1.981	0.042	CH <sub>2</sub> Cl <sub>2</sub> <sup>h</sup>	34a
{( $\mu$ -L)[Cu(Ph <sub>2</sub> P(CH <sub>2</sub> ) <sub>6</sub> PPh <sub>2</sub> ) <sub>2</sub> ] <sub>2</sub> } <sup>•+</sup>	2.0050	2.0134	2.0047	1.9968	0.0166	<i>i</i>	35

<sup>a</sup> At 298 K. <sup>b</sup> At 110 K. <sup>c</sup>  $A_{iso} = 3.5$  mT. <sup>d</sup>  $A_1 = 6.1$  mT. <sup>e</sup>  $A_2 = 4.2$  mT. <sup>f</sup> Hyperfine structure from ligand. <sup>g</sup> Not determined. <sup>h</sup>  $g$  tensor components measured in toluene/dichloromethane (1:1). <sup>i</sup> Acetone/ethanol (5:1).

**Table 7.** UV/Vis/NIR Data for [(C<sub>6</sub>Me<sub>6</sub>)OsCl( $\mu$ -*abpy*)ClOs(C<sub>6</sub>Me<sub>6</sub>)]<sup>2+</sup> and Reduction Products<sup>a</sup>

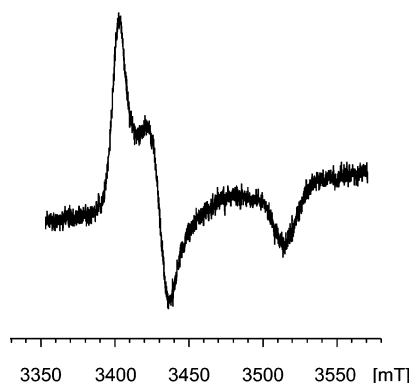
complex	$\lambda_{max}$ [nm] ( $\epsilon \times 10^{-3}$ [M <sup>−1</sup> cm <sup>−1</sup> ])	assignment
[(C <sub>6</sub> Me <sub>6</sub> )OsCl( $\mu$ - <i>abpy</i> )ClOs(C <sub>6</sub> Me <sub>6</sub> )] <sup>2+</sup>	291 (12.8)	IL
	321sh	
	414 (10.2)	$\pi$ - $\pi^*$
	662sh, 731 (12.3) <sup>b</sup>	<sup>1</sup> LLCT/MLCT
	883 (3.7), 974 (3.8) <sup>c</sup>	<sup>3</sup> LLCT/MLCT
[(C <sub>6</sub> Me <sub>6</sub> )OsCl( $\mu$ - <i>abpy</i> )ClOs(C <sub>6</sub> Me <sub>6</sub> )] <sup>•+</sup>	298 (11.1)	IL
	322sh	IL
	375 (10.5)	
	496 (6.0), 524 (6.2) <sup>d</sup>	IL
	705 (4.2)	MLCT
[(C <sub>6</sub> Me <sub>6</sub> )Os( $\mu$ - <i>abpy</i> )ClOs(C <sub>6</sub> Me <sub>6</sub> )] <sup>+</sup>	794(2.8), 902(2.1) <sup>e</sup>	SOMO-LUMO
	288 (17.0)	IL
	338sh	
[(C <sub>6</sub> Me <sub>6</sub> )Os( $\mu$ - <i>abpy</i> )Os(C <sub>6</sub> Me <sub>6</sub> )]	509(6.7), 542(7.2) <sup>f</sup>	MLCT/ $\pi$ - $\pi^*$
	290 (18.3)	IL
	358 (11.9)	IL
	509 (5.9)	
	654 (6.7)	MLCT II/ $\pi$ - $\pi^*$
	895 (4.0), 1009 (8.9) <sup>g</sup>	MLCT I

<sup>a</sup> From spectroelectrochemistry in DMF/0.1 M Bu<sub>4</sub>NPF<sub>6</sub>. <sup>b</sup> Vibrational structuring  $\Delta\nu = 1425$  cm<sup>−1</sup>. <sup>c</sup> Vibrational structuring  $\Delta\nu = 1038$  cm<sup>−1</sup>. <sup>d</sup> Vibrational structuring  $\Delta\nu = 1077$  cm<sup>−1</sup>. <sup>e</sup> Vibrational structuring  $\Delta\nu = 1507$  cm<sup>−1</sup>. <sup>f</sup> Vibrational structuring  $\Delta\nu = 1196$  cm<sup>−1</sup>. <sup>g</sup> Vibrational structuring  $\Delta\nu = 1262$  cm<sup>−1</sup>.

**Figure 5.** X band (9.5953 GHz) EPR spectrum of {( $\mu$ -*abpy*)[(C<sub>6</sub>Me<sub>6</sub>)OsCl]<sub>2</sub>}(PF<sub>6</sub>) (**2a**) in 0.1 M Bu<sub>4</sub>NPF<sub>6</sub>/DMF at 110 K.

as the differences between *abpy*- and *bpy*m-bridged analogues.

The stability of various redox states of **2**, especially the isolability of the one-electron-reduced form **2a**, allowed us to carry out more detailed investigations by EPR and UV/vis spectroelectrochemistry. In DMF solution at 298 K complex **2a** exhibits a <sup>189</sup>Os metal isotope

**Figure 6.** W band (94.261 GHz) EPR spectrum of {( $\mu$ -*abpy*)[(C<sub>6</sub>Me<sub>6</sub>)OsCl]<sub>2</sub>}(PF<sub>6</sub>) (**2a**) in 0.1 M Bu<sub>4</sub>NPF<sub>6</sub>/DMF at 80 K.

hyperfine splitting (Figure 4, Table 6). This isotope with  $I = 3/2$  has 16.1% natural abundance, which leads to the occurrence of the following isotope combinations in a symmetrically dinuclear compound (Os: isotope without nuclear spin): 3% <sup>189</sup>Os/<sup>189</sup>Os, 27% <sup>189</sup>Os/Os, and 70% Os/Os. Relative to the isotropic hyperfine coupling constant  $a_{iso} = 471$  mT<sup>28</sup> the value of 3.5 mT for **2a** signifies a still small but noticeable participation of the heavy metal centers at the SOMO.

Further information could be expected from low-temperature spectra in frozen solution; however, the metal hyperfine signals in the standard X band EPR spectrum (9.5 GHz) caused sufficient overlap (Figure 5) as to preclude immediate analysis. We therefore resorted to EPR spectroscopy in the W band (94 GHz),

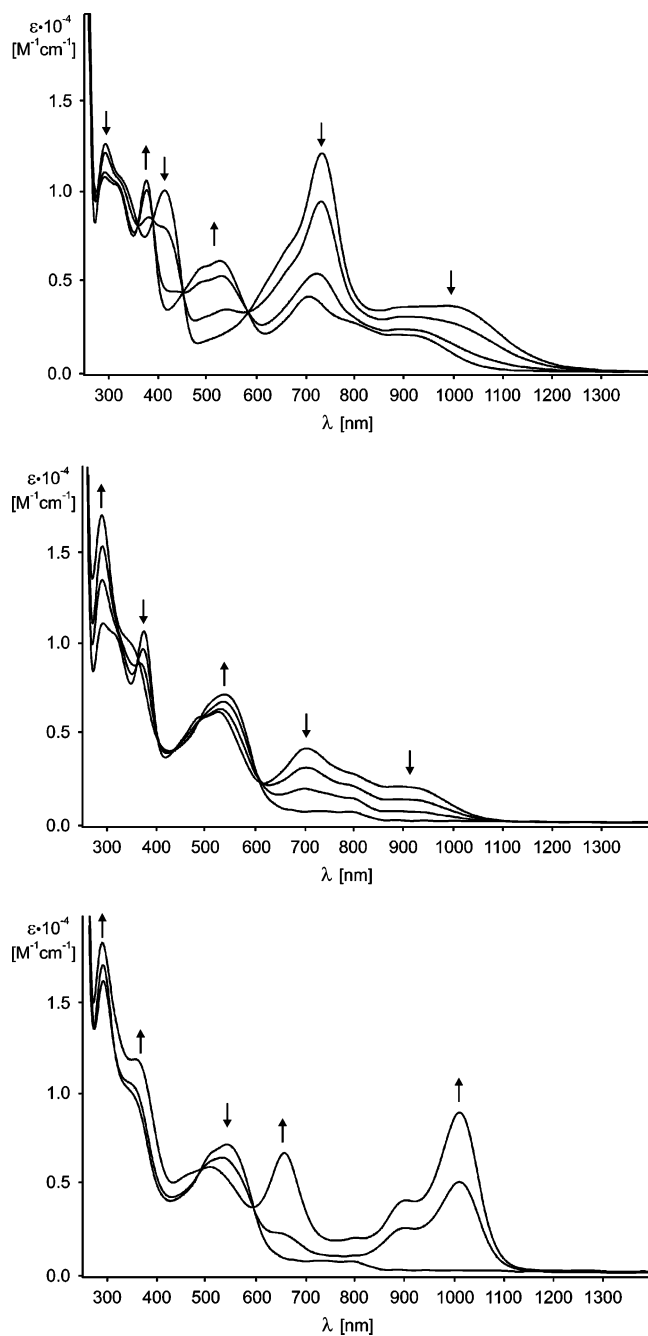


**Figure 7.** Spectroelectrochemical response on reduction of  $\{(\mu\text{-abpy})[(\text{C}_6\text{Me}_6)\text{OsCl}]_2\}^{2+}$  (**2b**) to  $\{(\mu\text{-abpy})[(\text{C}_6\text{Me}_6)\text{OsCl}]_2\}^{+}$  (**2a**) (top) and then via  $[(\text{C}_6\text{Me}_6)\text{Os}(\mu\text{-abpy})\text{ClOs}(\text{C}_6\text{Me}_6)]^+$  (center) to  $\{(\mu\text{-abpy})[(\text{C}_6\text{Me}_6)\text{Os}]_2\}$  (bottom) in 0.1 M  $\text{Bu}_4\text{NPF}_6/\text{DMF}$ .

which helps to considerably separate the  $g$  components (Figure 6). Combining the information from both the X and W band spectra we could thus straightforwardly analyze the spectrum with the data summarized in Table 6. As for the mononuclear radical complex, both the considerable deviation of  $g_{\text{iso}}$  from 2 and the high  $g$

anisotropy  $\Delta g = g_1 - g_3$  are caused by the strong spin-orbit coupling effects from divalent osmium.<sup>28,29</sup> The slightly rhombic  $g$  anisotropy is evident from the W band spectrum measured in frozen solution (Figure 6). Previous high-frequency EPR studies of dinuclear complexes with the abpy radical anion have also shown a tendency for rhombic symmetry.<sup>13,34a,35</sup> Two of the anisotropic coupling constants for  $^{189}\text{Os}$  could be directly determined (Figure 6); they are in agreement with the isotropic value of 3.5 mT.

UV/vis spectroelectrochemistry using an OTTLE cell was used to characterize not only **2b** and **2a** but also further reduced species (Scheme 2). The spectrum of the starting system **2b** is once more dominated by the singlet and (weaker, bathochromically shifted) triplet charge transfer transitions involving the 5d element with its high spin-orbit coupling constant (Figure 7, Table 7).<sup>13,29</sup> Reduction results in a shift and intensity loss of the CT bands while transitions at about 500 nm, attributed to the abpy radical anion,<sup>19a</sup> become observable. The first EC reduction to the formally diosmium(0,II) species  $[(\text{C}_6\text{Me}_6)\text{Os}(\mu\text{-abpy})\text{OsCl}(\text{C}_6\text{Me}_6)]^+$  produces the expected emergence of a band in the visible above 500 nm, which is further intensified and bathochromically shifted to 1010 nm after the second (E)EC process (Figure 7, Table 7), leading to the “diosmium(0)” system  $[(\text{C}_6\text{Me}_6)\text{Os}(\mu\text{-abpy})\text{Os}(\text{C}_6\text{Me}_6)]$ . The apparent vibrational structuring of this intense band ( $\Delta\nu = 1270 \text{ cm}^{-1}$ ) indicates strong mixing between the metal  $d_{xz}$  orbitals and the  $\pi^*$  MO of the acceptor ligand, to the extent that charge transfer designations based on oxidation state assignments become less meaningful. The conspicuous intense band at 1010 nm may thus be attributed to a transition between highly mixed  $d_{\pi}(\text{Os})$  and  $\pi^*(\text{abpy})$  orbitals.

In conclusion, the presented results have confirmed not only the remarkable capacity of the abpy bridging ligand to strongly couple organometallic reaction centers<sup>13b,26</sup> but also the extraordinary response of  $[(\text{C}_6\text{Me}_6)\text{ClOs}]^+$  in relation to  $[(\text{C}_5\text{Me}_5)\text{ClM}]^+$  ( $\text{M} = \text{Rh}$ , or  $\text{Ir}$ ) and the enormous  $\pi$  donor effect of the resulting  $(\text{C}_6\text{Me}_6)\text{Os}$  fragment. The coupling of reversible electron transfer and bond-breaking processes should make the results more relevant for general chemistry; for instance, these observations may have implications for the unusual chemistry of areneosmium compounds in stabilizing carbene and allenylidene ligands as described recently.<sup>37</sup>

**Acknowledgment.** This work was supported by a grant from the Deutsche Forschungsgemeinschaft (DFG), by the Stuttgart Graduate College on “Magnetic Resonance”, and by the Fonds der Chemischen Industrie.

OM049085T

(37) (a) Weberndörfer, B.; Henig, G.; Hockless, D. C. R.; Bennett, M. A.; Werner, H. *Organometallics* **2003**, *22*, 744–758. (b) Weberndörfer, B.; Werner, H. *J. Chem. Soc., Dalton Trans.* **2002**, 1479–1486.